AAPM Report No. 204

Size-Specific Dose Estimates (SSDE) in Pediatric and Adult Body CT Examinations

Report of AAPM Task Group 204, developed in collaboration with the International Commission on Radiation Units and Measurements (ICRU) and the Image Gently campaign of the Alliance for Radiation Safety in Pediatric Imaging

DISCLAIMER: This publication is based on sources and information believed to be reliable, but the AAPM, the authors, and the publisher disclaim any warranty or liability based on or relating to the contents of this publication.

The AAPM does not endorse any products, manufacturers, or suppliers. Nothing in this publication should be interpreted as implying such endorsement.

ISBN: 978-1-936366-08-8
ISSN: 0271-7344

Published by
American Association of Physicists in Medicine
One Physics Ellipse
College Park, MD 20740-3846

Size-Specific Dose Estimates (SSDE) in Pediatric and Adult Body CT Examinations

Report of AAPM Task Group 204

Members

John M. Boone‡* (Co-Chair)
The University of California, Davis

Keith J. Strauss‡† (Co-Chair)
Children's Hospital, Boston

Dianna D. Cody‡
M.D. Anderson Cancer Center, Houston

Cynthia H. McCollough‡*
Mayo Clinic, Rochester

Michael F. McNitt-Gray‡*
The University of California, Los Angeles

Thomas L. Toth‡
General Electric Healthcare, Waukesha

Consultants

Marilyn J. Goske†, M.D.
Cincinnati Children's Hospital Medical Center, Cincinnati, OH

Donald P. Frush†, M.D.
Duke University, Durham

‡American Association of Physicists in Medicine (AAPM)
*International Commission on Radiation Units and Measurements (ICRU), CT Committee
†Image Gently campaign of the Alliance for Radiation Safety in Pediatric Imaging

Contents

1. Introduction

There are approximately 80 million CT examinations performed in the United States annually. About 7 million of these occur on children (Mettler 2000). In response to this, the Society for Pediatric Radiology (SPR) sponsored a conference on this topic in 2001 (Slovis 2002, Berdon 2002) which was followed by a conference in 2002 sponsored by the National Council on Radiation Protection and Measurements (Linton 2003). In 2008, the Alliance for Radiation Safety in Pediatric Imaging ("Alliance") was founded by the American Association of Physicists in Medicine (AAPM), the American College of Radiology (ACR), the American Society of Radiologic Technologists (ASRT) and the Society for Pediatric Radiology (SPR) to address the unique needs of imaging children when using ionizing radiation. Currently, the Alliance represents over 60 affiliated organizations (at least 20 are international) representing over 750,000 people working in medical imaging. The Alliance promotes radiation protection for children through an awareness, education, and advocacy-based social marketing campaign (Image Gently). The Alliance strives to foster justification (examination indicated) and optimization (appropriate balance between radiation dose and study quality) for every pediatric CT examination. In order to achieve this balance, pediatric radiologists, medical physicists and radiologic technologists need user-friendly computational tools to estimate radiation dose during pediatric CT examinations. The methods provided in this document are designed to provide such tools, not only for pediatric CT, but for CT examinations of patients of any size.

Current CT scanners display the volume computed tomography dose index ($CTDI_{vol}$) and the dose length product (DLP) dose indices (Shope 1981, Dixon 2003, Boone 2007, McCollough 2008, McNitt-Gray 2002, AAPM 2008), both before and after the CT scan is performed. This has been required of manufacturers since 2002 (IEC 2002). $CTDI_{vol}$ was developed to provide a standardized method to compare *radiation output levels* between different CT scanners using a reference phantom. DLP, which is the product of $CTDI_{vol}$ (mGy) and scan length (cm), is related to the total ionizing energy imparted to the reference phantom. Both $CTDI_{vol}$ and DLP are sensitive to changes in scan parameters such as tube voltage, tube current, gantry rotation time, pitch, and bowtie filter, but are independent of patient size. The $CTDI_{vol}$ is determined for either a 16 cm or 32 cm diameter polymethyl methacrylate (PMMA) cylindrical reference phantom, often called the "head" or "body" CTDI phantom, respectively.

For a given patient's CT scan, the $CTDI_{vol}$ and the related DLP are displayed for a reference phantom (i.e., head or body CTDI phantom), the diameter of which (i.e., 16 cm or 32 cm) is selected by the scanner. In general, for exams using a head bow-tie filter or head scan protocol, the 16 cm diameter phantom is used. For exams of the torso, when a body bow-tie filter or body scan protocol is used, the 32 cm diameter phantom is used. At present, for pediatric body CT protocols, some manufacturers use the 16 cm diameter phantom and some use the 32 cm diameter phantom as the reference for calculating $CTDI_{vol}$ and DLP. To accurately interpret $CTDI_{vol}$ or DLP for an individual patient, or to compare to other reported values, the phantom diameter used for a specific *scanner model and software version* must be known. In most cases, the phantom diameter used is now displayed on the user console along with $CTDI_{vol}$ and DLP, or is present in the DICOM Dose Report. Older scanner models and software versions, however, may lack this information in a readily accessible place and the scanner manufacturer representative should be consulted in such case.

The dose received by a patient from a CT scan is dependent on both patient size and scanner radiation output. $CTDI_{vol}$ provides information regarding *only* the scanner output. It does not address patient size, and hence does not estimate patient dose (McCollough 2011). This is a concern, *because for smaller pediatric patients, interpreting the displayed $CTDI_{vol}$ (or DLP) as patient dose—without recognizing the distinction between the two—could lead to underestimating patient dose levels by a factor of 2–3 if the 32 cm PMMA phantom was used for reference.*

This task group was charged with developing conversion factors that can be applied to the displayed $CTDI_{vol}$ dose index to allow practitioners to be able to estimate patient dose. These factors take into account patient size, and hence are especially important for pediatric CT or when small adults are scanned. The work presented here was specifically motivated by the needs of the Alliance (Strauss 2009), but also reflects ongoing, independent research performed by a number of research groups around the United States. The scope of this task group is limited to estimating patient dose using scanner output ($CTDI_{vol}$) and factors associated with patient size. Other differences between the current CT scanner radiation output indices and patient dose estimates due to the use of "short" phantoms (15 cm along the *z*-axis) for $CTDI_{vol}$ measurements (Dixon 2003, 2006; Boone 2007) are not addressed by this task group.

2. Methods

The $CTDI_{vol}$ is the parameter which is used to normalize the conversion factors to as described in this document, and so we start with a detailed description of how the $CTDI_{vol}$ is computed.

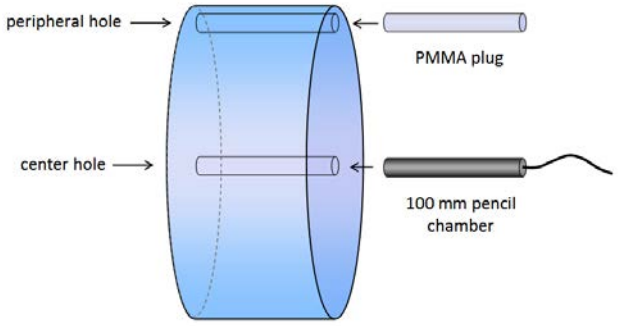

Figure 1. The general methodology for the assessment of $CTDI_{100}$ is illustrated. The 100 mm long pencil chamber is placed either at the center or at the periphery of a polymethyl methacrylate dose phantom. There are two standard PMMA phantoms, 16 cm and 32 cm in diameter and both are 15 cm in length. Unused holes are plugged with PMMA rods. The $CTDI_{100}$ methods are used to compute $CTDI_{vol}$, as described in the text.

Definitions: $CTDI_{vol}$

The $CTDI_{vol}$ parameter displayed on most CT scanner consoles is measured following standard protocols (McCollough 2008, Bauhs 2008). The $CTDI_{100}$ is defined as:

$$CTDI_{100} = \frac{1}{nT}\int_{z=-50mm}^{+50mm} D(z)\ dz\,. \qquad \text{Equation 1}$$

The measurement approach is illustrated in Figure 1. $CTDI_{100}$ can be measured at the center of the phantom and at the periphery, resulting in $CTDI_{100}^{center}$ for the center and $CTDI_{100}^{periphery}$ for the peripheral measurement. It is emphasized that the quantity measured for $CTDI_{100}$ defined in this document is air kerma, represented in the units of mGy. There is no conversion to dose in tissue or in PMMA using f-factors or their SI equivalent, as prescribed in earlier definitions of CTDI (e.g., $CTDI_{FDA}$).

However, for measurements made in units of exposure (roentgen), a conversion from exposure to air kerma (mGy) is required: Exposure (R) x 8.73 = Air Kerma (mGy).

The weighted CTDI, $CTDI_w$, is computed as:

$$CTDI_w = \frac{1}{3} CTDI_{100}^{center} + \frac{2}{3} CTDI_{100}^{periphery}. \quad \text{Equation 2}$$

Recognizing that dose in CT is inversely related to helical (spiral) pitch, the $CTDI_{vol}$ is defined as:

$$CTDI_{vol} = \frac{CTDI_w}{pitch}, \quad \text{Equation 3}$$

where pitch is defined as the ratio of the table feed (in mm) per 360° gantry rotation to the nominal collimated beam width (nT in Equation 1, in mm).

Definitions: Size related parameters

Figure 2. The anterior posterior (AP) and lateral dimension, along with effective diameter are illustrated in this figure. The lateral dimension can be determined from a PA or AP CT radiograph, and the AP dimension can be determined by a lateral CT radiograph. The effective diameter corresponds to a circle having an area equal to that of the patient's cross section on a CT image. Some investigators have also used patient perimeter (circumference) as a metric of patient size.

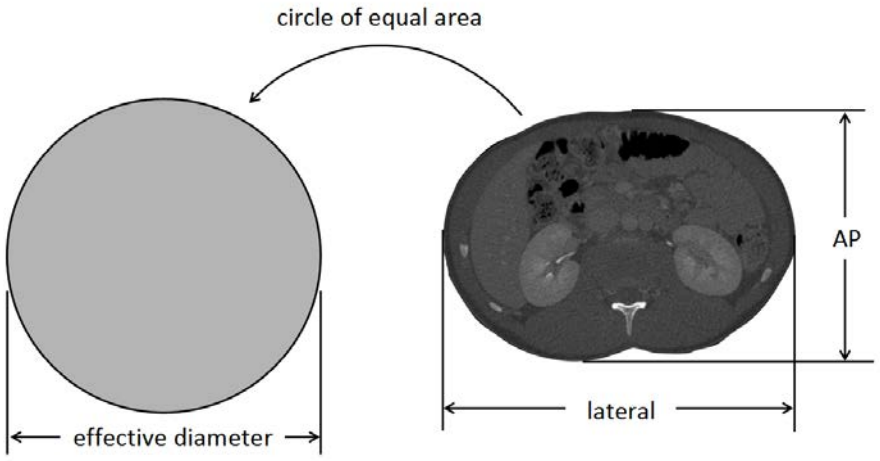

Figure 2 illustrates several of the parameters discussed in this section. The CT radiograph is the scanned projection radiography used in CT to prescribe the scan range (also called Scout™, Topogram™ and Scanogram™ by various manufacturers).

Lateral Dimension: The lateral (LAT) dimension is the side-to-side (left to right) dimension of the body part being scanned. This dimension can be assessed using electronic calipers on the standard PA CT radiograph that is acquired in most cases prior to a CT scan. In the absence of a CT radiograph, the lateral dimension could be determined using physical patient calipers, which are sometimes available in a radiology facility.

AP Dimension: Anterior-posterior dimension is the thickness of the body part of the patient being scanned in the anterior-posterior dimension, for example from the surface of the stomach to the surface of the back. To measure the AP dimension from a CT radiograph, a lateral projection would be necessary. The AP dimension can be easily measured using digital calipers on a conventional

lateral CT radiograph, which is acquired prior to the CT scan under some circumstances. In the absence of a measurement from a CT radiograph, physical calipers can be used to make this measurement.

AP + Lat dimension: This parameter is the sum of the lateral and AP dimensions. The analyses performed for this report have shown that the sum of these two orthogonal dimensions is linearly related to the effective diameter.

Effective Diameter: The effective diameter represents the diameter of the patient at a given location along the z-axis of the patient (in the cranialcaudal dimension), assuming that the patient has a circular cross section. While some body parts approximate a circular section, many do not. The effective diameter can be thought of as the diameter of the circle whose *area* is the same as that of the patient cross section (Figure 2). To calculate this from the known AP and lateral dimensions, the patient is assumed to be elliptical in cross section, with the radii r_1 and r_2 being:

$$r_1 = \frac{LAT}{2} \qquad \text{Equation 4.1}$$

$$r_2 = \frac{AP}{2}. \qquad \text{Equation 4.2}$$

The area, *A*, of the ellipse is computed using:

$$A = \pi r_1 r_2 . \qquad \text{Equation 5}$$

From the area of the patient's cross section, *A*, the effective diameter is computed as:

$$effective\ diameter = 2\sqrt{\frac{A}{\pi}} . \qquad \text{Equation 6}$$

Combining Equations 4 through 6, it can be seen that:

$$effective\ diameter = \sqrt{AP \times LAT} . \qquad \text{Equation 7}$$

Overall Approach

It has been shown that a patient size-dependent factor can be used to estimate patient dose from scanner output indices (e.g. $CTDI_{vol}$) for patients of different sizes. The size dependent factor can be used over a range of patient sizes, and extends to large patients as well as small patients. Because of the general availability of the $CTDI_{vol}$ parameter on the CT console, the methods employed by the various investigators all rely on normalization by $CTDI_{vol}$, as conventionally measured using either the 16 or 32 cm diameter PMMA phantoms. This normalization process factors out most differences between individual scanners and tube potential settings (Turner 2010, 2011). Since most modern CT scans can display $CTDI_{vol}$ ***prior*** to the CT scan of a given patient, the proposed factors can be used by the CT technologist at the CT console to estimate dose *prior* to the CT scan.

2.1 Methods for Different Groups

The various tools used by the four independent research groups are illustrated Figure 3.

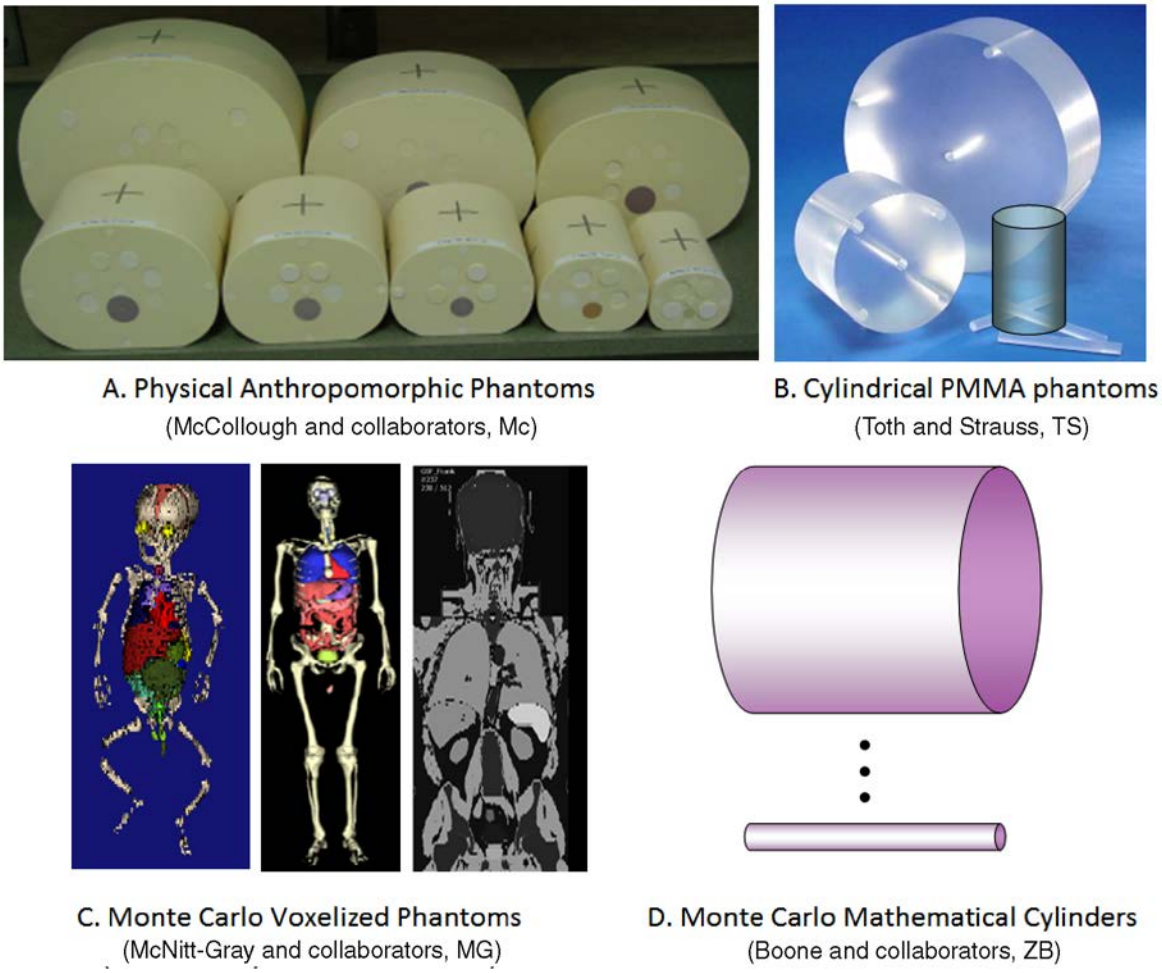

Figure 3. The various tools used by the four independent research groups: (A) McCollough and colleagues (Mc) performed physical dose measurements using a series of eight anthropomorphic tissue-equivalent phantoms. (B) Toth and Strauss (TS) used two existing cylindrical PMMA phantoms, the 16 and 32 cm diameter CTDI phantoms, and a third 10 cm diameter phantom. (C) McNitt-Gray and colleagues (MG) performed Monte Carlo dose calculations using a series of seven anthropomorphic mathematical phantoms, of which three are shown here. (D) Boone and colleagues (ZB) used Monte Carlo calculations on a series of cylinders of different diameter with different compositions.

For this report, we have combined data from four different groups of investigators who have independently been studying the potential of patient size-dependent factors to estimate patient dose from $CTDI_{vol}$. While this compendium of results is not a meta-analysis *per se*, the excellent consistency between the results of the independent research groups suggests a level of confidence in the derived factors greater than if only one group produced the data. Serendipitously, two of the groups made use of Monte Carlo–based measurements, while the other two engaged in physical measurements on phantoms, and this broadens the experimental methodology used to arrive at the recommended conversion factors.

2.1.1. Physical Measurements using Anthropomorphic Phantoms (McCollough and colleagues "Mc")

McCollough et al., at the Mayo Clinic (Rochester, MN) used a set of eight tissue-equivalent anthropomorphic torso phantoms (CIRS, Norfolk, VA) spanning a range of sizes from newborn (LAT dimension 9 cm) to large adult (LAT dimension 39 cm, Figure 3A). With the exception of the newborn phantom, the aspect ratios of these phantoms were very similar. To represent patients with different body shapes (e.g. more round than oval), three additional phantoms were created by adding tissue-equivalent material on top of the CIRS phantoms: a rounder new born, 15 years old, and large adult. AP and lateral dimensions, perimeter, and area were determined for each of the 11 phantoms.

Phantoms were scanned using four different CT scanner models: Sensation 16 and Definition (Siemens Healthcare, Forchheim, Germany) and LightSpeed Ultra and VCT (GE Healthcare, Milwaukee, WI). Exposure was measured according to the methods of AAPM TG-111 (AAPM 2010) using a 0.6cc ion chamber (Radcal, Monrovia, CA) and converted to dose to tissue (mGy) using an f-factor of 1.073 mGy [dose] / mGy [air kerma] or 9.37 mGy/R.

Dose in CT depends on the amount of scatter produced within the scanned object. Hence, the use of phantoms having only a 15 cm length along the z-axis would underestimate the dose to actual patients. To provide a realistic scattering environment, a human torso was simulated by placing additional phantoms with similar attenuation properties directly adjacent to the CIRS phantom along the longitudinal direction. The scan length for an abdominal CT scan for each torso phantom was estimated based upon clinical experience, and each phantom was scanned using helical (spiral), axial (sequential), and cine (perfusion) scan protocols. Measurements were made at the center of the field-of-view and four peripheral positions, and a mean dose over the field-of-view calculated using a 1/3 center and 2/3 peripheral average approach (i.e., Eqn 2). Mean dose was divided by $CTDI_{vol}$ at every patient size.

2.1.2. Physical Measurements Using Cylindrical PMMA Phantoms (Toth and Strauss "TS")

Toth and Strauss (TS) used x-ray attenuation, expressed in terms of a water-equivalent diameter (Huda 2000, Menke 2005) to describe patient size for the standard 15 cm long, 16 cm diameter, and 32 cm diameter PMMA phantoms, and a 15 cm long, 10 cm diameter PMMA cylinder (Figure 3B).

Toth and Strauss measured standard $CTDI_{vol}$ for 16- and 64-slice CT scanners from Philips, GE, Toshiba, and Siemens across a range of kV values from 80 kV to 140 kV. Regression models of the $CTDI_{vol}$ measurements, normalized to the 16 and 32 cm diameter phantom measurements, were obtained as a function of the phantom's water-equivalent diameter. The water-equivalent diameters for a cohort of head, chest, and body pediatric patients were also determined from CT radiographs and CT images as well as measurement of the patient's lateral dimension using electronic calipers. Using the regression models, tables of normalized $CTDI_{vol}$ as a function of patient lateral dimension were developed. The result is a set of scale factors that estimate the dose for a 15 cm long phantom having the same water-equivalent x-ray attenuation as the patient.

2.1.3. Monte Carlo Measurements on Voxelized Phantoms (McNitt-Gray and colleagues "MG")

The McNitt-Gray laboratory at UCLA used Monte Carlo simulation techniques to study the effects of patient size on organ dose for abdominal CT exams (Turner 2011). Multi-detector CT (MDCT)

scanners from each of the major manufacturers were simulated using the "equivalent source" method described by Turner et al. (Turner 2009). A cohort of eight voxelized patient models, known as the GSF patient models (Petoussi-Henss 2005) were used to represent a range of sizes from newborn to large adult that included males and females. Simulated abdominal CT exams were performed for all patient models on each scanner model. The scan length simulated was proportional to the scan length typical for each body size simulated, and this ranged from 15 cm to 33 cm. All organ doses were obtained using a previously described MDCT simulation approach (DeMarco 2005) built on the MCNPX (Monte Carlo N-Particle eXtended v2.7.a) radiation transport code (Waters 2002, 2003).

The scanner-specific organ doses were normalized by corresponding $CTDI_{vol}$ values and averaged across scanners to obtain scanner-independent organ dose per $CTDI_{vol}$ coefficients for each patient model. To obtain a metric for patient size, the outer perimeter of each patient was measured at the central slice of the abdominal scan region. Then, the relationship between organ dose per $CTDI_{vol}$ coefficients and patient perimeter was investigated for organs that were directly irradiated by the abdominal scan.

2.1.4. Monte Carlo Measurements on Simple Cylindrical Phantoms (Zhou and Boone "ZB")

Zhou and Boone at the University of California Davis used the SIERRA Monte Carlo code system, developed by Boone (Boone 2000A) and previously reported (Zhou 2008) to compute dose to infinitely long cylinders of different compositions (water, PMMA, and polyethylene) with diameters ranging from 1 cm to 50 cm, in 22 different increments. The geometry and bow tie filters of the GE Lightspeed 16 scanner were used in the simulations. The monoenergetic simulation data (8 keV–140 keV) were incorporated into several spreadsheet calculation tools (Excel, Microsoft Corporation, Redmond, WA). A spectral model (Boone 1997) was incorporated into the calculation tool as well, allowing the user to adjust the spectrum from 40 kV to 140 kV, and put in any amount of added aluminum or copper filtration. The polyenergetic spectrum was produced by spectrally weighting the monoenergetic data compiled in the spreadsheet. In this study, x-ray spectra at 80, 100, 120, and 140 kV were simulated with 9.8 mm of added Al filtration. These spectra delivered half-value layers (in Al) of 5.8 mm, 7.1 mm, 8.0 mm, and 8.8 mm for 80 kV, 100 kV, 120 kV, and 140 kV, respectively.

The spreadsheet allows the computation of dose in the material (water, PMMA, or polyethylene) at the center and the peripheral holes in the mathematical cylindrical phantom. The data used a water-equivalent phantom and were combined using a 1/3 center and 2/3 peripheral average (i.e., Eqn 2), to estimate the absorbed dose to the patient. The study reported in the literature (Zhou 2008) only discussed a scatter integration length of 100 mm; however separate spreadsheet tools were also developed for a 10 mm scatter integration width as well as an infinite scatter integration width. To simulate the dose for realistic scan lengths in this study, the 100 mm scan length data were averaged with the infinite scan length data, and to estimate the dose typical for a 20–30 cm scan length, which is similar to the values used by the other contributors in this report.

For normalization, the Monte Carlo determined air kerma values for the 16 cm and 32 cm PMMA phantoms were used, identical to the protocol for physically measuring $CTDI_{vol}$ as discussed previously. The dose in water (or tissue) was computed as a function of cylindrical diameter and was normalized (divided) by the $CTDI_{vol}$ computed (or measured) in air. Hence, the f-factor for water (or

tissue) was implicitly included in these results. This essentially is an f-factor of approximately 1.073 mGy [dose] / mGy [air kerma] or 9.37 mGy / roentgen.

3. Results

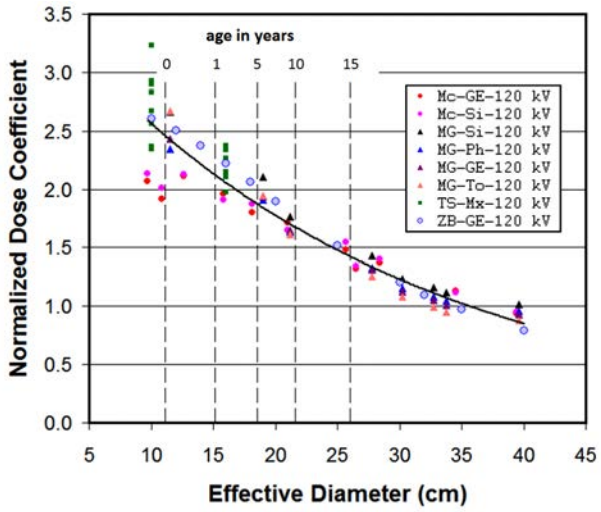

Figure 4. The normalized dose coefficient for the 32 cm PMMA $CTDI_{vol}$ phantom is shown as a function of effective diameter. The individual data points correspond to four independent research groups, as indicated in the key. (Mc=McCollough, MG=McNitt-Gray, TS=Toth/Strauss, ZB=Zhou/Boone). Scanners represented are also indicated in the key (GE=General Electric, Si=Siemens, Ph=Phillips, To=Toshiba, Mx=Mixed Scanner manufacturers).

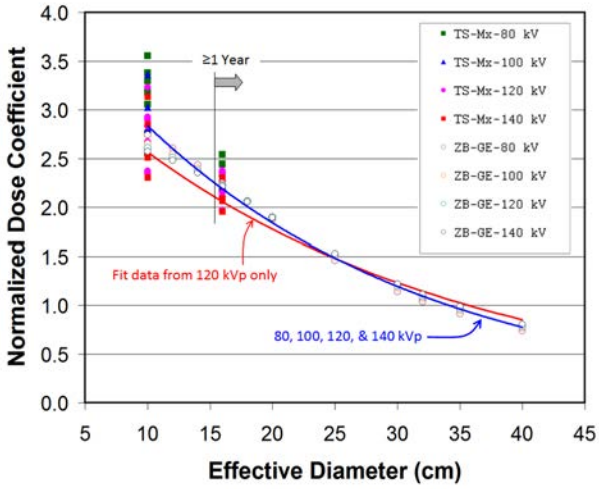

Figure 5. The normalized dose coefficient for the 32 cm PMMA $CTDI_{vol}$ phantom is shown as a function of effective diameter. Symbols correspond to a range of x-ray tube voltages from 80 kV to 140 kV. The best fit (blue) curve is shown. The best fit curve from Figure 4, representing 120 kV only, is superimposed on this plot (red, as labeled). Good correspondence is seen between these two curves. Refer to Figure 4 for legend descriptions.

Figure 4 illustrates the combined data from the four groups, where the 32 cm diameter PMMA phantom was used for the $CTDI_{vol}$ normalization. The data shown in this figure are for 120 kV only. The data from each group are indicated by a different symbol, as indicated in the key and caption. All plotted data points were combined and used in the computer fit assuming an exponential relationship ($Y = a\, e^{-bx}$) between the normalized dose coefficient and effective diameter. The computer fit is seen to accommodate most of the individual points quite well, with a correlation coefficient (r^2) of 0.942. The dashed vertical lines correspond to the effective diameters of children of different ages, as indicated on the figure. The data points corresponding to the 10 cm location on Figure 4 demonstrate slightly more variation than elsewhere on the curve. For this very small phantom, the increased variability may be due to increased dependency on spectral differences across scanner manufacturers.

The data compiled and demonstrated in Figure 4 represent the efforts of four groups, but primarily on abdominal/pelvic CT geometries where the torso dimensions are comprised mostly of soft tissue. In regards to thoracic CT, however, we refer to the work by Huda and coworkers (Huda 2000). In that work, patients who ranged in effective diameter from 12.2 cm to 28.6 cm were evaluated, and the correction factors computed from that data (6 data points) showed an average difference of 3.3% in comparison to the fit curve shown in Figure 4. The maximum difference was +16% for the smallest patient (12.2 cm). This comparison is made to demonstrate that the conversion factors presented here are reasonably applicable to chest, abdomen, and pelvic CT studies.

Figure 5 illustrates the normalized dose coefficient as a function of effective diameter for the Toth/Strauss (TS) and Zhou/Boone (ZB) data. The data points in Figure 5 cover x-ray tube voltages ranging from 80 kV to 140 kV. The ZB data represent computer simulations for a GE Lightspeed 16 scanner across 11 different cylinder diameters, while the TS data are indicative of physical measurements made at 3 different phantom diameters but across a total of 18 different CT scanner makes and models. The best-fit curve across all data points results in a correlation coefficient of 0.973. Superimposed on this figure is the best-fit curve from Figure 4, which represents the data points from all four groups but for only 120 kV. There is generally good agreement between the two curves, however there is some divergence toward smaller effective diameters. The equations and fit coefficients for all pertinent graphs are presented in Appendix A.

Averaged over all data points, the average percent difference for the absolute value of the differences between the two curves in Figure 5 is 5.1%. For the data ranging between an effective diameter of 10 cm and 32 cm, the average percent difference is 4.3%. Recognizing that a minority of pediatric CT patients are below one year of age, if we eliminate data for effective diameters below 15 cm, and include data for pediatric patients ranging from 15 cm to 32 cm in effective diameter, the average percent difference between the two curves is only 3.1%. The small difference between the curves determined at 120 kV and curves determined across all relevant CT kV's suggests that only one set of size-dependent factors is necessary across tube voltage and scanner manufacturer and model to estimate patient dose from $CTDI_{vol}$. Consequently, it was felt that the curve illustrated in Figure 4 is sufficiently robust to provide a single set of factors across both scanner type and tube potential. The fit for data from Figure 4 was used instead of that of Figure 5, because it represents a broader cross section of data from four independent groups. The fit coefficients for the curves seen in Figure 4, therefore, were used to generate the correction factors found in Table 1.

Figure 6 illustrates the normalized dose coefficient for the 16 cm PMMA $CTDI_{vol}$ data as a function of effective diameter at 120 kV, and includes data from three independent groups. Like the 32 cm phantom data seen in Figure 4, the best-fit curve across all data points in Figure 6 also shows excellent agreement, with a correlation coefficient of 0.967. Due to this excellent fit, and for the same reasons discussed in the above paragraph, this fit data was used to generate the dose correction coefficients appropriate to the 16 cm PMMA phantom. These data sets are presented in Table 2.

Table 1. This table provides conversion factors based on the use of the 32 cm diameter PMMA phantom for $CTDI_{vol}$. Table 1A shows the conversion factor as a function of the sum of the lateral and AP dimensions. Table 1B shows conversion factors as a function of the lateral dimension, and Table 1C is for the AP dimension. Table 1D provides conversion factors as a function of effective diameter. It is essential that these data be used when the $CTDI_{vol}$ reported is known to be based on the 32 cm diameter body dosimetry phantom.

Table 1A

Lat+AP Dim (cm)	Effective Dia (cm)	Conversion Factor
16	7.7	2.79
18	8.7	2.69
20	9.7	2.59
22	10.7	2.50
24	11.7	2.41
26	12.7	2.32
28	13.7	2.24
30	14.7	2.16
32	15.7	2.08
34	16.7	2.01
36	17.6	1.94
38	18.6	1.87
40	19.6	1.80
42	20.6	1.74
44	21.6	1.67
46	22.6	1.62
48	23.6	1.56
50	24.6	1.50
52	25.6	1.45
54	26.6	1.40
56	27.6	1.35
58	28.6	1.30
60	29.6	1.25
62	30.5	1.21
64	31.5	1.16
66	32.5	1.12
68	33.5	1.08

Table 1B

Lateral Dim (cm)	Effective Dia (cm)	Conversion Factor
8	9.2	2.65
9	9.7	2.60
10	10.2	2.55
11	10.7	2.50
12	11.3	2.45
13	11.8	2.40
14	12.4	2.35
15	13.1	2.29
16	13.7	2.24
17	14.3	2.19
18	15.0	2.13
19	15.7	2.08
20	16.4	2.03
21	17.2	1.97
22	17.9	1.92
23	18.7	1.86
24	19.5	1.81
25	20.3	1.76
26	21.1	1.70
27	22.0	1.65
28	22.9	1.60
29	23.8	1.55
30	24.7	1.50
31	25.6	1.45
32	26.6	1.40
33	27.6	1.35
34	28.6	1.30

Table 1C

AP Dim (cm)	Effective Dia (cm)	Conversion Factor
8	8.8	2.68
9	10.2	2.55
10	11.6	2.42
11	13.0	2.30
12	14.4	2.18
13	15.7	2.08
14	17.0	1.98
15	18.3	1.89
16	19.6	1.81
17	20.8	1.73
18	22.0	1.65
19	23.2	1.58
20	24.3	1.52
21	25.5	1.45
22	26.6	1.40
23	27.6	1.34
24	28.7	1.29
25	29.7	1.25
26	30.7	1.20
27	31.6	1.16
28	32.6	1.12
29	33.5	1.08
30	34.4	1.05
31	35.2	1.02
32	36.0	0.99
33	36.8	0.96
34	37.6	0.93

Table 1D

Effective Dia (cm)	Conversion Factor
8	2.76
9	2.66
10	2.57
11	2.47
12	2.38
13	2.30
14	2.22
15	2.14
16	2.06
17	1.98
18	1.91
19	1.84
20	1.78
21	1.71
22	1.65
23	1.59
24	1.53
25	1.48
26	1.43
27	1.37
28	1.32
29	1.28
30	1.23
31	1.19
32	1.14
33	1.10
34	1.06

Lat+AP	Effective	Conversion
Dim (cm)	Dia (cm)	Factor
70	34.5	1.04
72	35.5	1.01
74	36.5	0.97
76	37.5	0.94
78	38.5	0.90
80	39.5	0.87
82	40.5	0.84
84	41.5	0.81
86	42.4	0.78
88	43.4	0.75
90	44.4	0.72

Lateral	Effective	Conversion
Dim (cm)	Dia (cm)	Factor
35	29.6	1.25
36	30.6	1.20
37	31.7	1.16
38	32.7	1.11
39	33.8	1.07
40	34.9	1.03
41	36.1	0.98
42	37.2	0.94
43	38.4	0.90
44	39.6	0.87
45	40.8	0.83

AP	Effective	Conversion
Dim (cm)	Dia (cm)	Factor
35	38.4	0.91
36	39.1	0.88
37	39.8	0.86
38	40.4	0.84
39	41.1	0.82
40	41.7	0.80
41	42.3	0.78
42	42.8	0.77
43	43.4	0.75
44	43.9	0.74
45	44.4	0.73

Effective	Conversion
Dia (cm)	Factor
35	1.02
36	0.99
37	0.95
38	0.92
39	0.88
40	0.85
41	082
42	0.79
43	0.76
44	0.74
45	0.71

Table 2. This table provides conversion factors based on the use of the 16 cm diameter PMMA phantom for $CTDI_{vol}$. Table 2A shows the conversion factor as a function of the sum of the lateral and AP dimensions. Table 2B shows conversion factors as a function of the lateral dimension, and Table 2C is for the AP dimension. Table 2D provides conversion factors as a function of effective diameter. It is essential that these data be used when the $CTDI_{vol}$ reported is known to be based on the 16 cm diameter body dosimetry phantom.

Table 2A

Lat + AP Dim (cm)	Effective Dia (cm)	Conversion Factor
12	5.7	1.50
13	6.2	1.47
14	6.7	1.44
15	7.2	1.42
16	7.7	1.39
17	8.2	1.36
18	8.7	1.34
19	9.2	1.31
20	9.7	1.29
21	10.2	1.26
22	10.7	1.24
23	11.2	1.22
24	11.7	1.19
25	12.2	1.17
26	12.7	1.15
27	13.2	1.13
28	13.7	1.10
29	14.2	1.08
30	14.7	1.06
31	15.2	1.04
32	15.7	1.02
33	16.2	1.00
34	16.7	0.98
35	17.2	0.97
36	17.6	0.95
37	18.1	0.93

Table 2B

Lateral Dim (cm)	Effective Dia (cm)	Conversion Factor
6	8.2	1.36
7	8.7	1.34
8	9.2	1.32
9	9.7	1.29
10	10.2	1.26
11	10.7	1.24
12	11.3	1.21
13	11.8	1.19
14	12.4	1.16
15	13.1	1.13
16	13.7	1.10
17	14.3	1.08
18	15.0	1.05
19	15.7	1.02
20	16.4	0.99
21	17.2	0.96
22	17.9	0.94
23	18.7	0.91
24	19.5	0.88
25	20.3	0.85
26	21.1	0.83
27	22.0	0.80
28	22.9	0.77
29	23.8	0.75
30	24.7	0.72
31	25.6	0.70

Table 2C

AP Dim (cm)	Effective Dia (cm)	Conversion Factor
6	5.8	1.50
7	7.3	1.41
8	8.8	1.33
9	10.2	1.26
10	11.6	1.19
11	13.0	1.13
12	14.4	1.07
13	15.7	1.02
14	17.0	0.97
15	18.3	0.92
16	19.6	0.88
17	20.8	0.84
18	22.0	0.80
19	23.2	0.76
20	24.3	0.73
21	25.5	0.70
22	26.6	0.67
23	27.6	0.64
24	28.7	0.62
25	29.7	0.59
26	30.7	0.57
27	31.6	0.55
28	32.6	0.53
29	33.5	0.51
30	34.4	0.50
31	35.2	0.48

Table 2D

Effective Dia (cm)	Conversion Factor
6	1.49
7	1.43
8	1.38
9	1.32
10	1.27
11	1.22
12	1.18
13	1.13
14	1.09
15	1.05
16	1.01
17	0.97
18	0.93
19	0.90
20	0.86
21	0.83
22	0.80
23	0.77
24	0.74
25	0.71
26	0.69
27	0.66
28	0.63
29	0.61
30	0.59
31	0.56

Lat + AP	Effective	Conversion
Dim (cm)	Dia (cm)	Factor
38	18.6	0.91
39	19.1	0.89
40	19.6	0.88
42	20.6	0.84
44	21.6	0.81
46	22.6	0.78
48	23.6	0.75
50	24.6	0.72
52	25.6	0.70
54	26.6	0.67
56	27.6	0.64
58	28.6	0.62
60	29.6	0.60
62	30.5	0.57
64	31.5	0.55
66	32.5	0.53
68	33.5	0.51
70	34.5	0.49
72	35.5	0.47
74	36.5	0.46
76	37.5	0.44
78	38.5	0.42
80	39.5	0.41
82	40.5	0.39

Lateral	Effective	Conversion
Dim (cm)	Dia (cm)	Factor
32	26.6	0.67
33	27.6	0.65
34	28.6	0.62
35	29.6	0.60
36	30.6	0.57
37	31.7	0.55
38	32.7	0.53
39	33.8	0.51
40	34.9	0.48
41	36.1	0.46
42	37.2	0.44
43	38.4	0.42
44	39.6	0.40
45	40.8	0.39
46	42.1	0.37
47	43.3	0.35
48	44.6	0.33
49	45.9	0.32
50	47.2	0.30
51	48.5	0.29
52	49.9	0.27
53	51.3	0.26
54	52.7	0.24
55	54.1	0.23

AP	Effective	Conversion
Dim (cm)	Dia (cm)	Factor
32	36.0	0.46
33	36.8	0.45
34	37.6	0.44
35	38.4	0.42
36	39.1	0.41
37	39.8	0.40
38	40.4	0.39
39	41.1	0.38
40	41.7	0.37
41	42.3	0.36
42	42.8	0.36
43	43.4	0.35
44	43.9	0.34
45	44.4	0.34
46	44.8	0.33
47	45.2	0.33
48	45.6	0.32
49	46.0	0.32
50	46.4	0.31
51	46.7	0.31
52	47.0	0.30
53	47.2	0.30
54	47.5	0.30
55	47.7	0.30

Effective	Conversion
Dia (cm)	Factor
32	0.54
33	0.52
34	0.50
35	0.48
36	0.47
37	0.45
38	0.43
39	0.41
40	040
41	0.38
42	0.37
43	0.35
44	0.34
45	0.33
46	0.32
47	0.30
48	0.29
49	0.28
50	0.27
51	0.26
52	0.25
53	0.24
54	0.23
55	0.22

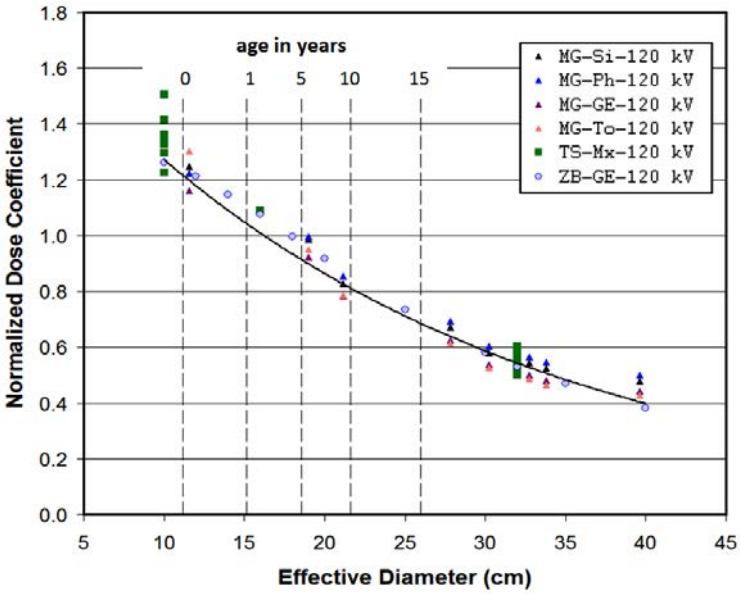

Figure 6. The normalized dose coefficient is shown as a function of effective diameter, here for $CTDI_{vol}$ measurements made using the **16 cm diameter** PMMA $CTDI_{vol}$ phantom at 120 kV. For the smaller phantom, the magnitude of the conversion coefficients is smaller. This is because for the same scanner output, $CTDI_{100}$ measurements made using the smaller 16 cm diameter phantom result in a numerically larger values for $CTDI_{vol}$.

Figures 4, 5, and 6 all use the effective diameter as the dependent variable; however the actual effective diameter is usually not known prior to the CT scan. From the CT radiograph, however, either the AP dimension or the lateral dimension can be determined from the digital calipers on the CT scanner console. Alternately, the AP or lateral dimension of the patient can be physically measured using calipers designed for this purpose. Because of the general availability of either the AP dimension or the lateral dimension (or both) from the CT radiograph, it is useful to understand the relationship between these dimensions and the effective diameter.

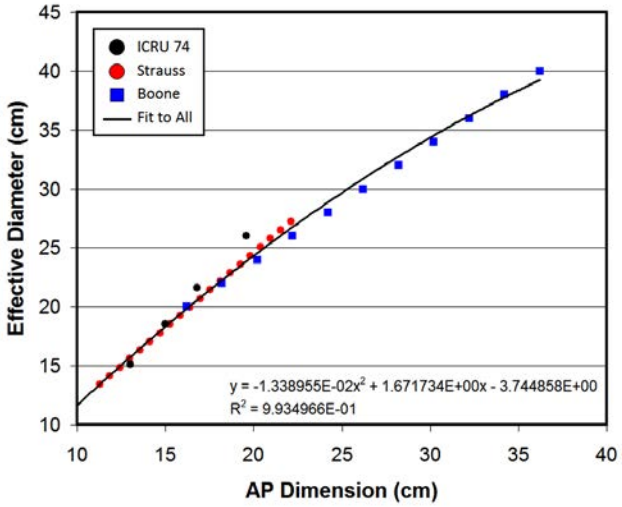

Figure 7. The effective diameter as a function of AP dimension is illustrated. The data points from three sources were used, as indicated in the key. A slight downward curvature is seen in this relationship.

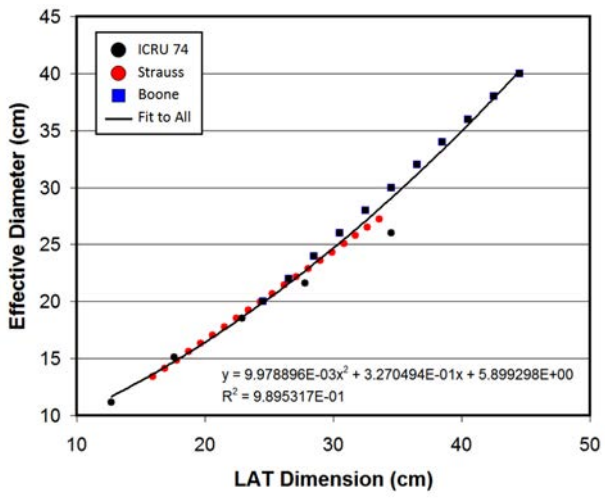

Figure 8. The effective diameter as a function of lateral dimension of the patient is illustrated in this figure. Here, a slight upward curvature is seen.

Figure 7 illustrates the effective diameter of the abdomen as a function of the AP dimension of the patient, over a large range of patient sizes. The data in this figure come from three sources: tabulated data from ICRU 74, data measured from CT images in a pediatric hospital setting (Kleinman 2010),

and data measured by Boone (Boone 2000B) using CT images in an adult imaging environment. The best-fit curve using a second order polynomial across all data points demonstrates an excellent correlation coefficient of $r^2 = 0.993$. For these data, the slope of the curve slightly decreases as a function of AP dimension, resulting in a slight downward curvature in the plot.

Figure 8 illustrates the effective diameter as a function of lateral dimension, from the same three data sources as indicated for Figure 7. Here, a second order polynomial fitting function also shows excellent fit with $r^2 = 0.989$. In this case, however, the slope of the line increases as a function of lateral dimension, resulting in a slight upward curvature in the graph.

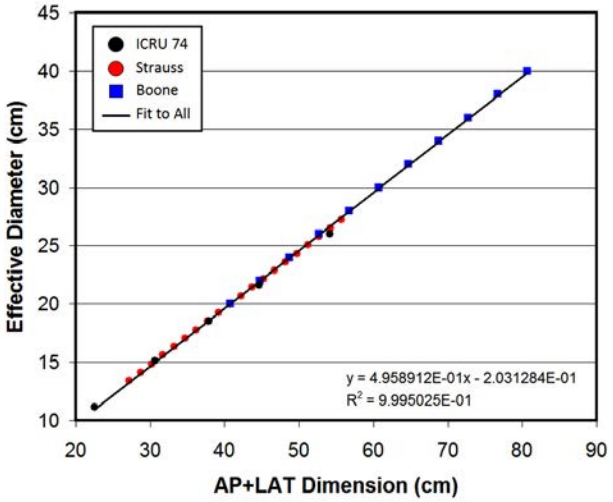

Figure 9. The effective diameter is shown as a function of the sum of the anterior posterior and lateral dimensions of the patient. The upward and downward curvatures illustrated in Figures 7 and 8 apparently compensate for each other, resulting in the linear relationship seen here.

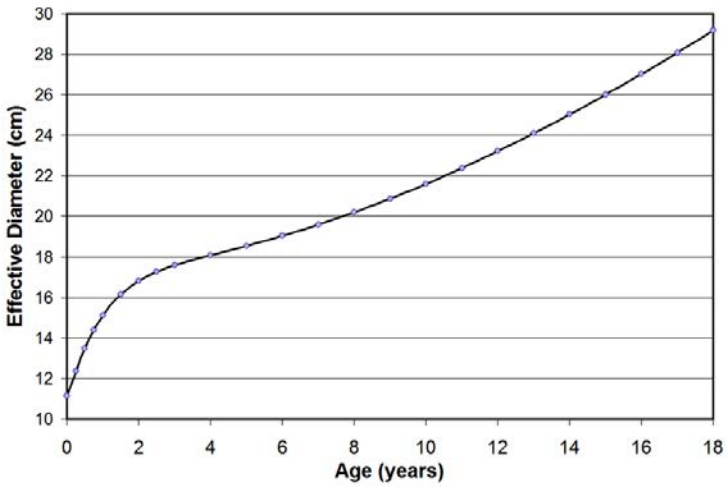

Figure 10. The effective diameter (in cm) is shown as a function of age (years). These data were computer fit using the data provided in ICRU 74. These data are listed in Table 3 as well.

In the event that both the AP and lateral dimensions of the patient are known, the sum of these two dimensions can be used to estimate effective diameter. This relationship is illustrated in Figure 9. Using data from three sources as discussed previously, a linear relationship is observed with an excellent correlation coefficient of 0.999. It is interesting to note that this parameter demonstrates a decidedly linear relationship with the effective diameter. Thus, the upward curvature associated with the lateral dimension (Figure 8) combines with the downward curvature associated with the AP dimension (Figure 7) to produce this linear relationship.

The fit equations shown in Figures 7–9 were used to generate Tables 1 and 2, where one can use any of the four different input variables (the sum of the AP and lateral dimensions, the AP dimension, the lateral dimension, or the effective diameter) to estimate the size-dependent conversion factor.

When the patient dimensions are not known, either from the cross-sectional CT images or a CT radiograph, the patient age may be known. Figure 10 provides the ICRU 74 data showing the relationship of patient effective diameter to age. These data can be used to convert age to effective diameter, which in turn can be used in Table 1D or 2D to estimate the size-dependent factor to estimate patient dose from $CTDI_{vol}$. While age may be used as an approximation, dose estimates

based on patient size are considered more accurate and should be used when size information is available.

Table 3. This table provides the ability to estimate effective diameter as a function of patient age (ICRU 74). Because there is large variability in patient size at the same age, age should be used only when size-based variables (provided in Tables 1 and 2) are not available. When using age, find the corresponding effective diameter in this table, and then refer that to either Table 1D (body phantom) or Table 2D (head phantom) to find the most appropriate conversion factor.

Patient Age (years)	Effective Diameter (cm)
0.0	11.2
0.2	12.1
0.4	13.1
0.6	13.9
0.8	14.6
1.0	15.1
1.2	15.6
1.4	16.0
1.6	16.3
1.8	16.6
2.0	16.8
2.5	17.3
3.0	17.6
3.5	17.9
4.0	18.1
4.5	18.3
5.0	18.5
6.0	19.0
7.0	19.6
8.0	20.2
9.0	20.9
10.0	21.6
11.0	22.4
12.0	23.2
13.0	24.1
14.0	25.0
15.0	26.0
16.0	27.0
17.0	28.1
18.0	29.2

4. Discussion

Two tables of conversion factors have been generated as a result of this work, Tables 1 and Table 2. Table 1 provides size-dependent factors to be applied to $CTDI_{vol}$, when the operator knows that the reference phantom used for reporting that $CTDI_{vol}$ value is measured using a 32 cm diameter PMMA CTDI phantom. Table 2 is to be used when the 16 cm PMMA dose phantom is used. In general, the factors are greater than unity for effective diameters smaller than the reference phantom (i.e., 32 cm in Table 1, 16 cm in Table 2), and are lower than unity for larger patients. For both Table 1 and 2, there are sections A through D, allowing the user to determine which metric to use to describe the approximate size of the patient—the LAT dimension can be used, the AP dimension, the sum of AP and lateral dimensions, or the effective diameter directly—which table is used depends on what data are available to the user.

It is recommended that the table to be used should be determined by the radiologists and or medical physicists working at an institution, and once the protocol is determined, the larger tables should be trimmed to only include the parameters of interest at a given institution—for example, if the standard protocol for pediatric body CT at an institution is to acquire a PA CT radiograph, then only the lateral dimension information would be available to the CT technologist using the digital calipers on the scanner—in this example, perhaps only Table 1B and 2B should be available at the scanner console, so that the incorrect table is not inadvertently used in the busy clinical setting.

Further, for a given scanner model and software version, it should be determined whether that scanner uses a 16 cm or 32 cm diameter PMMA phantom for its $CTDI_{vol}$ reporting for each CT protocol —If in doubt, contact the scanner manufacturer through their service representative and find out. Once the correct reference phantom size is determined for each scanner at the institution, use only one table—able 1 for the case of the 32 cm diameter phantom, and Table 2 for the 16 cm diameter phantom, for that scanner. In general, most scanners use the 32 cm PMMA for $CTDI_{vol}$ reporting on all (adult and pediatric) body protocols, but a few scanner types use the 16 cm data for pediatric body protocols.

5. Limitations

The data used to generate the curves corresponding to the data in Tables 1 and 2 were compiled from four different independent research groups. Despite the relatively good agreement between the data, slightly different methods were utilized in each of the independent groups. While the tables address patient cross-sectional size, all of the data leading to Tables 1 and 2 were generated using CT scan lengths in the range from 15 cm to 30 cm for phantoms of differing dimensions along the longitudinal axis (patient height). Because CT dose is a function of scan length and patient height, the actual patient dose resulting from significantly different scan lengths or patient heights may differ from that estimated using the accompanying tables. The methods described in this document either specifically modeled the abdominal region or used homogeneous cylinders, however comparisons with thoracic CT data from Huda (Huda 2000) show that the results provided here are consistent with thoracic CT as well as abdominal and pelvic CT geometries.

This report describes a method to *estimate* patient dose from $CTDI_{vol}$ that is reasonable for use in CT examinations of the torso (chest—abdomen and or pelvis). This report also did not address radiation dose associated with the CT radiograph. In addition, errors may occur in regards to how the patient

dimensions are determined. For example, if the lateral dimension is determined from the CT radiograph, a patient closer to the x-ray source will project a larger image than if positioned farther from the x-ray source, due to magnification issues. Thus, values derived from use of the factors in Tables 1 and 2 should always be considered as estimates of patient dose, and will be most accurate when the patient is centered in the gantry.

Many CT imaging protocols require the use of intravenous contrast agents. Often multiple scans are made at the same time on the same patient—for instance, pre-and post-contrast imaging. The radiation dose to the same region of the patient is the sum of the dose from all the CT scans covering that region. Of course, the absorbed dose from adjacent CT procedures (e.g., abdomen and pelvis) do NOT add.

The dose estimates using $CTDI_{vol}$, coupled with the conversion factors provided in Tables 1 or 2, provides an estimate of the dose at the center of the scanned region (along *z*) in the patient. This value will be slightly higher than the dose averaged over the entire tissue volume scanned. The dose is lower at the beginning of the scan volume, rises to a peak in the center of the scan volume, and then declines again at the end of the scan volume; therefore the average of the entire scan is slightly lower than the peak value estimated using the provided tables, which occurs at the middle of the scan volume.

6. Nomenclature

This report represents the recommendations of AAPM Task Group 204, as well as the CT report committee of the International Commission on Radiation Units and Measurements (ICRU) and the Alliance for Radiation Safety in Pediatric Imaging (parent group for the *Image Gently* campaign). It was felt necessary that specific nomenclature be suggested in regards to the proposed size-dependent conversion factors and the estimated doses that are produced from these factors. The intent is to permit concise reference to "doses" that are estimated using the methods outlined in this report. In the clinical environment (such as in the radiologist's dictated report), non-technical language is necessary. However, in the medical physics community, specific terminology is essential to clearly define the dose measurement methodology. We address both needs in this section.

The ***size-specific dose estimate*** (SSDE) is defined in this report as a patient dose estimate which takes into consideration corrections based on the size of the patient, using linear dimensions measured on the patient or patient images. The SSDE values discussed in this report are specifically based on the $CTDI_{vol}$ reported on CT scanners; however future modifications may include SSDE correction factors based on other pertinent phantom measurements. For example, CT measurements performed on different classes of CT phantoms (e.g., AAPM TG-200) and measurement protocols (e.g., AAPM Report 111) may provide the basis from which future SSDEs are built upon (AAPM 2010). In all cases, the SSDE should correspond to tissue doses, not air kerma or other quantities. Thus, the f-factors (air kerma to tissue dose correction values, formerly known as Roentgen to Rad conversion factors) should explicitly be a part of the SSDE metric.

Table 1 provides the size-dependent factors pertinent to the 32 cm diameter $CTDI_{vol}$ reference phantom; these factors can be represented as f_{size}^{32X}, where the *X* refers to the specific measure of size used, where *X* = *S* for the sum of AP and lateral dimension, *L* for lateral, *A* for AP, and *D* for

effective diameter. Thus, the *X* superscripts *S, L, A,* and *D* correspond to the conversion factors in Tables 1A, 1B, 1C, or 1D, respectively. So the nomenclature f_{size}^{32L} refers to the factor where a specific lateral dimension was used with Table 1B to assess the numerical value of the size-dependent factor. When spoken, we recommend the term "f-s coefficients" in referring to the conversion factors. It is noted that fit equations are provided in Appendix A, which also allow computation of the numerical values given in Tables 1A-D and 2A-D.

When the 16 cm diameter $CTDI_{vol}$ reference phantom is used, the factors are drawn from Table 2 and can be represented as f_{size}^{16X}, where *X* is defined as above.

The specific formula to estimate patient dose for a specific patient size is given by:

$$size\ specific\ dose\ estimate \quad = \quad SSDE \quad = \quad f_{size}^{32X} \quad \times \quad CTDI_{vol}^{32}, \qquad \text{Equation 8a}$$

for the 32 cm diameter $CTDI_{vol}$ reference phantom, and

$$size\ specific\ dose\ estimate \quad = \quad SSDE \quad = \quad f_{size}^{16X} \quad \times \quad CTDI_{vol}^{16} \qquad \text{Equation 8b}$$

for the 16 cm diameter $CTDI_{vol}$ reference phantom.

For clinical applications it is not suggested that the equations above be used, but rather that the term ***size-specific dose estimate*** or its acronym ***SSDE*** be used to indicate that patient size was taken into account according to the methods described in this report to estimate patient dose from the reported scanner output ($CTDI_{vol}$).

The SSDE should not be used to compute a modified dose length product (DLP). DLP = Scan Length (cm) × $CTDI_{vol}$ (mGy), and should not be used to compute effective dose E using *k*-factors.

7. Step-by-Step Example of Usage

Figure 11 shows two examples, illustrating the use of the size-dependent factors provided in this report.

Example 1: Dose estimate after the CT scan: Figure 11A illustrates a pediatric patient who was already scanned, and the dose estimate after the CT scan should be performed from the CT images, if available, as CT images have greater dimension accuracy compared to the CT radiographs. Using the digital calipers in the Picture Archiving and Communications in Medicine (PACS) system, the LAT dimension was measured to be 12.3 cm and the AP dimension was 9.9 cm. These two values sum to 22.2 cm. The $CTDI_{vol}$ for this CT scan was reported as 5.40 mGy for a 32 cm reference phantom. Table 1 is used when the reference phantom diameter is 32 cm. For a 22 cm sum of the AP and lateral dimensions, Table 1A shows a correction factor (f_{size}^{32S}) of 2.5. Therefore, the size-specific dose estimate (SSDE) for this patient is calculated as:

$$5.40\,mGy \quad \times \quad 2.50 \quad = \quad 13\,mGy\,.$$

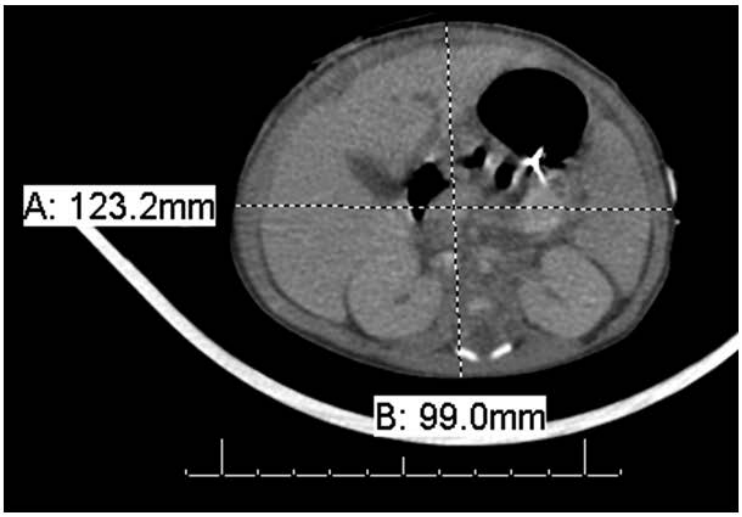

5.40 mGy = CTDIvol (32 cm phantom)

Figure 11A

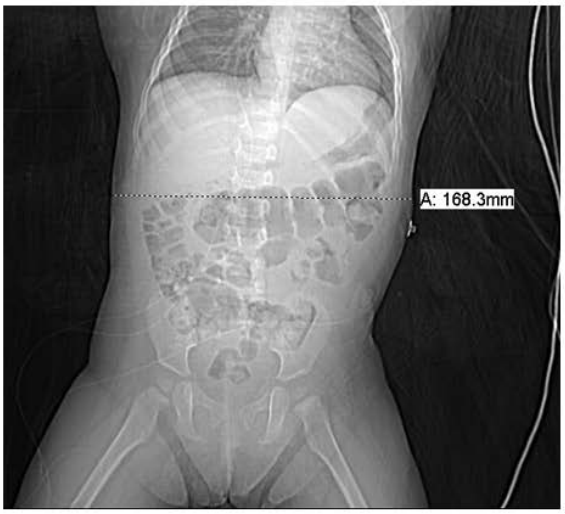

9.29 mGy = CTDIvol (16 cm phantom)

Figure 11B

Figure 11. Two cases used to illustrate size-specific dose estimation in CT. Figure 11A illustrates measurement of both the lateral and AP dimensions, and so the sum of these values is used with Table 1A to find the appropriate factor. In Figure 11B, the lateral dimension measured from the PA CT radiograph is used to find the conversion factor in Table 2B.

Example 2: Dose estimate prior to the CT scan: A PA CT radiograph was acquired (Figure 11B) and the digital calipers were used on the PA CT radiograph to measure a lateral dimension of about 16.8 cm. This measurement was made at the center (along the *z*-axis, which is defined as the cranial-caudal axis) of the anticipated CT field. The value of $CTDI_{vol}$ listed on the console was 9.29 mGy, and it is known that the 16 cm diameter PMMA phantom was the basis of the $CTDI_{vol}$ display for this protocol. When the 16 cm diameter PMMA phantom is used for determining the $CTDI_{vol}$ value, Table 2 should be used. Table 2B indicates that for a 17 cm lateral dimension, the correction factor (f_{size}^{16L}) is 1.08. Thus, the size-specific dose estimate (SSDE) for this patient is:

$$9.29\,mGy \quad \times \quad 1.08 \quad = \quad 10\,mGy\,.$$

8. Recommendations for Radiologist Reporting

Patient dose estimates are included in the radiology report in some practices. Suggested language for describing the size-specific dose estimates (SSDE) calculated using the methods in this report is given below:

The $CTDI_{vol}$ value reported on the scanner for the

[SELECT EITHER]

32 cm

16 cm

PMMA phantom was used with size-dependent factors obtained from AAPM Report 204. The factor for this patient was based on the patient's

[SELECT ONE OF THE FOLLOWING:]
AP dimension
lateral dimension
sum of the AP and lateral dimension
effective diameter.

Uncertainties associated with this method are approximately 20%. For this patient, the size-specific dose estimate (SSDE) for this CT scan is ____ mGy.

The language above was suggested by pediatric radiologists.

9. Summary

Given the relatively good agreement between the curves generated independently by four different research groups, the conversion factors provided in the accompanying tables should provide the radiologist, working with the CT technologist, the ability to estimate the average radiation dose to a volume of tissue for a given patient in a clinical setting. Using one or more of the patient size input parameters, it is anticipated that the size-specific dose estimate (SSDE) for each patient can be estimated prior to the CT scan.

It is recommended that when adjusting for the size of patients, that actual size metrics be used when possible. In some cases, size information is not available and only the patient's age is known. In this case, it is considered adequate to improve the dose estimate using the data shown in Figure 10, which illustrates effective diameter as a function of (average) patient age. Table 3 provides this same information in tabular format. However, it should be recognized that there are wide variations in the size of children at the same age, and so the dose conversion factors may be less accurate using this approach.

The methods provided in this document do not allow the estimation of organ doses *per se*, and in the absence of organ dose data it is not possible to infer effective dose (in mSv) from the methods described. For example, it is very important that the size specific dose estimate (SSDE) NOT be used when estimating effective dose in mSv using *k*-factors, using E (mSv) = $k \times$ DLP = $k \times$ Scan Length $\times$ $CTDI_{vol}$. The *k*-factors are based upon the Dose Length Product (DLP), which in turn includes $CTDI_{vol}$ in the product. The established *k*-factors (e.g., AAPM Report 96) (AAPM 2008) are based on computed organ dose data in adults, and it is likely that the organ dose distribution will be different in smaller patients—due to self attenuation issues and differences in how the beam shaping filter influences organ doses as a function of patient diameter. The SSDE metric improves the accuracy of the average dose estimate, but it does not correct for differences in the organ dose distribution. Therefore, the computation of effective dose is beyond the scope of this effort. In addition, the concept of effective dose was never intended to be applied on an individual patient basis. If risk assessment of a specific individual is required and the organ doses can be estimated, then the methods described in the BEIR VII report (BEIR VII) are recommended for risk estimation.

The primary purpose of this task group and this report was to give imaging providers, medical physicists, and CT technologists the ability to estimate radiation dose to patients, taking into account patient size, and using either the $CTDI_{vol}$ information on the scanner console or in the patient dose report. An improvement in dosimetry accuracy will result from the use of the accompanying tables,

compared to use of scanner output as a surrogate for patient dose. However, the resulting dose values must still be recognized as estimates only. It is likely that even when patient size is taken into account, the actual dose to any given patient may differ from the value calculated using this report by 10% to 20%. Because of this, it is essential to refer to the numbers generated using this document as dose *estimates*, and not as dose *calculations*. Users are also reminded to use an appropriate number of significant figures in reporting dose estimates. Specifically, it is suggested that for dose estimates above 5 mGy (e.g., 8 or 17 mGy) only integer values of dose estimates be reported and for dose estimates below 5 mGy (e.g., 3.6 or 4.7 mGy) only one digit beyond the decimal point be reported.

Appendix A: Pertinent Equations

There are several pertinent equations that describe the results of this work.

For Figures 4, 5, and 6, the exponential equation is given by:

$$y = a \times e^{-bx}, \qquad \text{Equation A-1}$$

where the coefficients are given in the table below:

Figure Number	X parameter	Y parameter	a	b
4	Eff. Diameter (cm)	Conversion Factor	3.704369	0.03671937
5	Eff. Diameter (cm)	Conversion Factor	4.378094	0.04331124
6	Eff. Diameter (cm)	Conversion Factor	1.874799	0.03871313

For Figures 7, 8, and 9, a second order polynomial equation is used. (The equation in Figure 9 is actually a first order polynomial equation—i.e., a linear fit). The equation is given by:

$$y = a + bx + cx^2, \qquad \text{Equation A-2}$$

where the values of the a, b, and c coefficients are given in the table below:

Figure Number	X parameter	Y parameter	a	b	c
7	AP diam (cm)	Eff. Diameter (cm)	–3.744858E0	1.671734E0	–1.338955E-2
8	LAT diam (cm)	Eff. Diameter (cm)	5.899298E0	3.270494E-1	9.978896E-3
9	AP + LAT diam (cm)	Eff. Diameter (cm)	–2.03128eE-1	4.958912E-1	0

The data shown in Figure 10 show the effective diameter as a function of patient, age, computed from ICRU 74. The computer fit for this relationship was given by:

$$y = a + b\,x^{1.5} + c\,x^{0.5} + d\,e^{-x} \qquad \text{Equation A-3}$$

where:
a = 18.788598
b = 0.19486455
c = –1.060056
d = –7.6244784.

References and Other Reading

AAPM 2008 — American Association of Physicists in Medicine (2008). The Measurement, Reporting and Management of Radiation Dose in CT (Report #96). AAPM Task Group 23 of the Diagnostic Imaging Council CT Committee. College Park, MD.

AAPM 2010 — American Association of Physicists in Medicine (2010). Comprehensive Methodology for the Evaluation of Radiation Dose in X-Ray Computed Tomography (Report #111). College Park, MD. (Implemented by TG-200)

Bauhs 2008 — Bauhs JA, Vrieze TJ, Primak AN, Bruesewitz MR, McCollough CH. CT dosimetry: comparison of measurement techniques and devices. *Radiographics*. 2008; 28(1):245-253. Review.

BEIR 7 — Health risks from exposure to low levels of ionizing radiation, BEIR VII phase 2, National Research Council, The National Academies Press, Washington, DC.

Berdon 2002 — Berdon WE, and Slovis TL. Where we are since ALARA and the series of articles on CT dose in children and risk of long-term cancers: what has changed? *Pediatr Radiol.* 2002; 32:699.

Boone 1997 — Boone JM, Seibert JA. An accurate method for computer-generating tungsten anode x-ray spectra from 30 kV to 140 kV. *Med Phys* 1997; 24:1661-1670.

Boone 2000A — Boone JM, Buonocore MH, Cooper VN III. Monte Carlo validation in diagnostic radiological imaging. *Med Phys.* 2000; 27:1294-1304.

Boone 2000B — Boone JM, Cooper VN, Nemzek WR, McGahan JP, Seibert JA. Monte Carlo assessment of computed tomography dose to tissue adjacent to the scanned volume. *Med Phys.* 2000; 27:2393-2407.

Boone 2007 — Boone, JM. The trouble with $CTDI_{100}$. *Med Phys.* 2007; 34(4):1364-1371.

Cody 2010 — Cody DD, Kim HJ, Cagnon CH, Larke FJ, McNitt-Gray MM, Kruger RL, Flynn MJ, Seibert JA, Judy PF, Wu X. Normalized CT dose index of the CT scanners used in the National Lung Screening Trial. *AJR Am J Roentgenol*. 2010 Jun; 194(6):1539-1546.

DeMarco 2005 — DeMarco JJ, Cagnon CH, Cody DD, Stevens DM, McCollough CH, O'Daniel J, McNitt-Gray MF. A Monte Carlo based method to estimate radiation dose from multidetector CT (MDCT): cylindrical and anthropomorphic phantoms. *Phys Med Biol*. 2005 Sep 7; 50(17):3989-4004.

DeMarco 2007 — DeMarco JJ, Cagnon CH, Cody DD, Stevens DM, McCollough CH, Zankl M, Angel E, McNitt-Gray MF. Estimating radiation doses from multidetector CT using Monte Carlo simulations: effects of different size voxelized patient models on magnitudes of organ and effective dose. *Phys Med Biol*. 2007 May 7; 52(9):2583-97.

Dixon 2003 — Dixon RL. A new look at CT dose measurement: Beyond CTDI. *Med Phys* 2003: 30(6):1272-1280.

Dixon 2006 — Dixon RL. Restructuring CT dosimetry—a realistic strategy for the future requiem for the pencil chamber. *Med Phys*. 2006; 33(10):3973-3976.

Huda 2000	Huda W, Scalzetti EM, Roskopf M. Effective doses to patients undergoing thoracic computed tomography examinations. *Med Phys.* 2000; 27 (5):838-844.
ICRU 74	Patient Dosimetry for X-Rays Used in Medical Imaging. *J. ICRU* Report 74; 2005. Appendix D, page 89.
IEC 2002	International Electrotechnical Commission (2002). Medical Electrical Equipment. Part 2-44: Particular requirements for the safety of x-ray equipment for computed tomography. IEC publication No. 60601-2-44. Ed. 2.1, International Electrotechnical Commission (IEC) Central Office: Geneva, Switzerland.
Jarry 2003	Jarry G, DeMarco JJ, Beifuss U, Cagnon CH, McNitt-Gray MF. A Monte Carlo-based method to estimate radiation dose from spiral CT: from phantom testing to patient-specific models. *Phys Med Biol.* 2003 Aug 21; 48(16):2645-2663.
Khursheed 2002	Khursheed A, Hillier MC, Shrimpton PC, and Wall BF. Influence of patient age on normalized effective doses calculated for CT examinations. *Br J Radiol.* 2002; 75:819-830.
Kleinman 2010	Kleinman PL, Strauss KJ, Zurakowski D, Bockley KS, Taylor GA. Patient size measured on CT images as a function of age at a tertiary care children's hospital. *AJR Am J Roentgenol.* 2010; 194(6):1611-1619.
Linton 2003	Linton OW, Mettler FA. National conference on dose reduction in CT, with an emphasis on pediatric patients. *AJR Am J Roentgenol.* 2003; 181:321-329.
Mathieu 2010	Mathieu KB, McNitt-Gray MF, Zhang D, Kim HJ, Cody DD. Precision of dosimetry-related measurements obtained on current multidetector computed tomography scanners. *Med Phys*. 2010 Aug; 37(8):4102-4109.
McCollough 2006	McCollough CH, Bruesewitz MR, Kofler JM Jr. CT dose reduction and dose management tools: overview of available options. *Radiographics*. 2006 Mar-Apr; 26(2):503-512. Review.
McCollough 2007	McCollough CH, Primak AN, Saba O, Bruder H, Stierstorfer K, Raupach R, Suess C, Schmidt B, Ohnesorge BM, Flohr TG. Dose performance of a 64-channel dual-source CT scanner. *Radiology*. 2007 Jun; 243(3):775-784. [Epub 2007 Apr 19].
McCollough 2008	McCollough CH. CT dose: how to measure, how to reduce. *Health Phys*. 2008 Nov; 95(5):508-517.
McCollough 2009	McCollough CH, Primak AN, Braun N, Kofler J, Yu L, Christner J. Strategies for reducing radiation dose in CT. *Radiol Clin North Am*. 2009 Jan; 47(1):27-40. Review.
McCollough 2011	McCollough CH, Leng S, Yu L, Cody DD, Boone JM, McNitt-Gray MF, CT Dose index and patient dose: they are not the same thing. *Radiology.* 2011; 259:311-316 (Editorial).
McNitt-Gray 2002	McNitt-Gray MF. AAPM/RSNA Physics Tutorial for Residents: Topics in CT. Radiation dose in CT. *Radiographics*. 2002 Nov-Dec; 22(6):1541-1553. Review.

Menke 2005	Menke, J. Comparison of different body size parameters for individual dose adaptation in body CT of adults. *Radiology*. 2005; 236:565–571.
Mettler 2000	Mettler FA Jr, Wiest PW, Locken JA, Kelsey CA. CT scanning: patterns of use and dose. *J Radiol Prot.* 2000; 20(4):353-359.
NCRP 160	Ionizing radiation exposure to the population of the United States, NCRP Report 160, Bethesda, MD, 2008.
Petoussi-Henss 2005	Petoussi-Henss N, Zankl M, Nosske D. Estimation of patient dose from radiopharmaceuticals using voxel models. *Cancer Biother Radiopharm*. 2005; 20(1):103-109.
Shope 1981	Shope T, Gagne R, and Johnson G. A method for describing the doses delivered by transmission x-ray computed tomography. *Med Phys*. 1981; 8:488-495.
Slovis 2002	Slovis, TL. The ALARA concept in pediatric CT: myth or reality? *Radiology.* 2002; 223:5-6.
Strauss 2009	Strauss KJ, Goske MJ, Frush DP, Butler PF, Morrison G. Image Gently Vendor Summit: working together for better estimates of pediatric radiation dose from CT. *AJR Am J Roentgenol*. 2009; 192(5):1169-1175.
Turner 2009	Turner AC, Zhang D, Kim HJ, DeMarco JJ, Cagnon CH, Angel E, Cody DD, Stevens DM, Primak AN, McCollough CH, McNitt-Gray MF. A method to generate equivalent energy spectra and filtration models based on measurement for multidetector CT Monte Carlo dosimetry simulations. *Med Phys*. 2009 Jun; 36(6):2154-2164.
Turner 2010	Turner AC, Zankl M, DeMarco JJ, Cagnon CH, Zhang D, Angel E, Cody DD, Stevens DM, McCollough CH, McNitt-Gray MF. The feasibility of a scanner-independent technique to estimate organ dose from MDCT scans: using $CTDI_{vol}$ to account for differences between scanners. *Med Phys*. 2010 Apr; 37(4):1816-1825.
Turner 2011	Turner A, Zhang D, Khatonabadi M, Zankl M, DeMarco J, Cagnon C, et al. The feasibility of patient size-corrected, scanner-independent organ dose estimates for abdominal CT exams. *Med Phys*. 2011; 38:820-829.
Waters 2002	Waters L. MCNPX User's Manual, Version 2.4.0 Los Alamos National Laboratory Report LA-CP-02-408. Los Alamos, NM, 2002.
Waters 2003	Waters L. MCNPX Version 2.5.C Los Alamos National Laboratory Report LA-UR-03-2202. Los Alamos, NM, 2003.
Yu 2009	Yu L, Li H, Fletcher JG, McCollough CH. Automatic selection of tube potential for radiation dose reduction in CT: a general strategy. *Med Phys*. 2010 Jan; 37(1):234-243.
Zhang 2009	Zhang D, Savandi AS, Demarco JJ, Cagnon CH, Angel E, Turner AC, Cody DD, Stevens DM, Primak AN, McCollough CH, McNitt-Gray MF. Variability of surface and center position radiation dose in MDCT: Monte Carlo simulations using CTDI and anthropomorphic phantoms. *Med Phys*. 2009 Mar; 36(3):1025-1038.

Zhou 2008 Zhou H, Boone JM, Monte Carlo evaluation of CTDI(infinity) in infinitely long cylinders of water, polyethylene, and PMMA with diameters from 10 mm to 500 mm. *Med Phys*. 2008; 35:2424-2431.